Enhancing Sensor Pattern Noise via Filtering Distortion Removal

Xufeng Lin, *Student Member, IEEE*, and Chang-Tsun Li, *Senior Member, IEEE*

***Abstract*—In this work, we propose a method to obtain higher quality sensor pattern noise (SPN) for identifying source cameras. We believe that some components of SPN have been severely contaminated by the errors introduced by denoising filters and the quality of SPN can be improved by abandoning those components. In our proposed method, some coefficients with higher denoising errors are abandoned in the wavelet representation of SPN and the remaining wavelet coefficients are further enhanced to suppress the scene details in the SPN. These two steps aim to provide better SPN with higher signal-to-noise ratio (SNR) and therefore improve the identification performance. The experimental results on 2,000 images captured by 10 cameras (each responsible for 200 images), show that our method achieves better receiver operating characteristic (ROC) performance when compared with some state-of-the-art methods.**

***Index Terms*—Correlation detection, denoising errors, digital forensics, sensor pattern noise, source camera identification.**

I. Introduction

SENSOR Pattern Noise (SPN) is a deterministic component remaining in the images taken by the imaging sensor. It mainly consists of the photo-response non-uniformity (PRNU) noise [1] arising primarily from the manufacturing imperfections and the inhomogeneity of silicon wafers. So unless otherwise specified in this paper, SPN refers to its main component, PRNU noise. The uniqueness to individual camera and stability against environmental conditions make SPN a feasible fingerprint for identifying source cameras. The use of SPN in identifying the source camera was first proposed by Lukas et al. in [1], where the reference SPN is first constructed for each camera by averaging the noise residuals extracted from images acquired by the camera. If the correlation between the noise residual of a query image (the query SPN) and the reference SPN is higher than a pre-defined threshold, the query image is deemed to be taken by the camera. However, the correlation-based detection of SPN heavily relies upon the quality of the extracted SPN, which can be severely contaminated by image content, color interpolation, JPEG compression and other non-unique artifacts. Therefore, exploring the way of extracting better SPN becomes of great significance for source camera identification.

Over the past few years, many methods have been proposed to enhance the quality of the SPN so as to improve the performance of source camera identification. In [2], Chen et al. proposed a maximum likelihood estimation (MLE) of the reference SPN from several residual images. Hu et al. [3] argued that the large or principal components of noise residue are more robust against random noise, so instead of using the full-length SPN, only a small portion of the largest components are involved in the calculation of correlation. Kang et al. [4] introduced a camera reference phase SPN to remove the periodic noise and other non-white noise contamination in the camera fingerprint. They proposed to use the correlation over circular cross-correlation norm (CCN) to further suppress the impact of periodic noise contamination. Actually, distortion to the SPN can be inflicted by each processing component of the imaging pipeline. We have done some work aiming at removing or suppressing the distortion resulting from different components in the image acquisition process. For example, based on the assumption that the stronger a signal component of SPN is, the more likely it is associated with strong scene details, Li [5] proposed six enhancing models to attenuate the interference from scene details. Afterwards, Li et al. [6] continued to propose a Color-Decoupled PRNU (CD-PRNU) extraction method to prevent the color filtering array (CFA) interpolation errors from propagating into the physical components. They extracted the PRNU from each color channel and then assembled them to get the more reliable CD-PRNU. In [7], Lin et at. proposed a novel spectrum equalization algorithm (SEA) to preprocess the reference SPN aiming at suppressing the non-unique artifacts introduced by CFA interpolation, JPEG compression and other periodic operations. It has better performance over the zero-mean (ZM) and Wiener filtering in DFT domain (WF) operations proposed in [2].

In this work, we propose a method for obtaining better SPN via filtering distortion removal (FDR). It is widely accepted that the choice of denoising filters is very important [3], [8], [9] and the quality of SPN can be improved by choosing better denoising filters. However, in their pursuit for better SPN, researchers usually ignore the fact that even the "best" denosing filter can inflict distortion on SPNs. As a result, some components of SPN may be severely contaminated by denoising errors and become uninformative. By abandoning the components that have been severely contaminated, SPN of better quality can be obtained. To the best of our knowledge, there is no existing work attempting to improve the quality of SPN through attenuating the errors introduced by the denoising filter.

Manuscript received September 10, 2015; revised December 20, 2015; accepted January 20, 2016. Date of publication January 25, 2016; date of current version February 09, 2016. This work was supported by the EU FP7 Digital Image Video Forensics project under Grant 251677, DIVeFor 251677, DIVeFor. The associate editor coordinating the review of this manuscript and approving it for publication was Prof. Vishal Monga.

The authors are with the Department of Computer Science, University of Warwick, Coventry CV4 7AL, U.K. (e-mail: xufeng.lin@warwick.ac.uk; C-T.Li@warwick.ac.uk).

Color versions of one or more of the figures in this paper are available online at http://ieeexplore.ieee.org.

Digital Object Identifier 10.1109/LSP.2016.2521349

The rest of this paper is organized as follows. In Section II, we will first revisit the expression of noise residue and analyze different parts of it, and then give the details of the proposed scheme. Experimental results and analyses will be presented in Section III. Finally, Section IV concludes the work.

II. Proposed Scheme

A. Motivation

Motivated by the work in [2], we start from the expression of noise residual $\mathbf{W}$, which is defined as the difference of the observed image $\mathbf{I}$ and its denoised version $\hat{\mathbf{I}}^{(0)} = F(\mathbf{I})$:

$$\begin{aligned} W &= \mathbf{I} - \hat{\mathbf{I}}^{(0)} \\ &= (\mathbf{1} + \mathrm{K})\mathbf{I}^{(0)} + \Theta - \hat{\mathbf{I}}^{(0)} \\ &= \mathrm{IK} + \mathbf{I}^{(0)} - \hat{\mathbf{I}}^{(0)} + (\mathrm{I}^{(0)} - \mathbf{I})\mathbf{K} + \Theta \\ &= \mathrm{IK} + \Xi, \end{aligned} \tag{1}$$

where $\mathbf{K}$ is the zero-mean like multiplicative factor responsible for PRNU, $\mathbf{I}^{(0)}$ is the noise-free image, $\boldsymbol{\Theta}$ stands for a complex of independent random noise components containing the interference from image content and other noises, $\boldsymbol{\Xi}$ is the sum of $\boldsymbol{\Theta}$ and the two additional terms introduced by the denoising filter. $\boldsymbol{\Xi}$ can be modeled as white Gaussain noise, which determines the accuracy of the estimation of $\mathbf{K}$. In [1], noise residues from a set of N images are averaged to suppress the random noise:

$$\mathbf{R}_f = \frac{1}{N}\sum_{i=1}^{N} \mathbf{W}_i, \tag{2}$$

where $\mathbf{R}_f$ serves as the reference SPN. Then the task of source camera identification is accomplished by calculating the normalized cross correlation (NCC) ρ between the noise residue $\mathbf{W}$ of the query image and the reference SPN $\mathbf{R}_f$:

$$\rho = corr(\mathbf{W}, \mathbf{R}_f) = \frac{(\mathbf{W} - \overline{\mathbf{W}}) \cdot (\mathbf{R}_f - \overline{\mathbf{R}}_f)}{\|\mathbf{W} - \overline{\mathbf{W}}\| \cdot \|\mathbf{R}_f - \overline{\mathbf{R}}_f\|}, \tag{3}$$

where $\|\cdot\|$ is the L_2 norm and the mean value is denoted with a bar. According to Equation (1), one possible way to improve the detection accuracy is to increase the signal-to-noise ratio (SNR) of the signal containing $\mathbf{K}$ in $\mathbf{W}$, which means we should promote $\mathbf{IK}$ and suppress $\boldsymbol{\Xi}$ as much as possible. For $\mathbf{IK}$, it is straightforward that the luminance $\mathbf{I}$ should be as high as possible. But as pointed out in [2], special attention should be paid to the saturated or dark image regions where $\mathbf{K}$ is absent or attenuated. While for $\boldsymbol{\Xi}$, it consists of three parts: $(\mathbf{I}^{(0)} - \mathbf{I})\mathbf{K}$, $\boldsymbol{\Theta}$ and $\mathbf{I}^{(0)} - \hat{\mathbf{I}}^{(0)}$. For the first term, as both the magnitudes of $\mathbf{K}$ and $\mathbf{I}^{(0)} - \mathbf{I}$ are very weak, the energy of $\boldsymbol{\Xi}$ is mostly concentrated in $\boldsymbol{\Theta}$ and $\mathbf{I}^{(0)} - \hat{\mathbf{I}}^{(0)}$. But since $\boldsymbol{\Theta}$ is a complex random noise term involving both the image content and the interferences from different stages of image acquisition process, so it is difficult to straightforwardly and properly model this part of signal. In spite of this, the scene details presented in $\boldsymbol{\Theta}$ can be more or less suppressed using the models proposed in [5]. For the third part of $\boldsymbol{\Xi}$, $\mathbf{I}^{(0)} - \hat{\mathbf{I}}^{(0)}$ is exactly the error introduced by the denoising filter. Therefore, choosing the SPN components with smaller denoising errors will hopefully provide better SPN with higher SNR. In the next sub-section, the denoising error will be analyzed quantitatively.

B. Denoising Error

As the most popular denoising filter for SPN extraction is the Mihcak filter proposed in [10], we will take this as an example. Assume the observed signal $g(k)$ (wavelet coefficients for $\mathbf{I}$) is the sum of the noise-free signal $f(k)$ (wavelet coefficients for $\mathbf{I}^{(0)}$) and a signal-independent additive random noise $v(k)$:

$$g(k) = f(k) + v(k), \tag{4}$$

where k is the index of wavelet coefficients. Considering a small region $N(k)$ in which the signal $f(k)$ is assumed to be stationary, $f(k)$ can be modeled as [11]:

$$f(k) = m_f + \sigma_f w(k), \tag{5}$$

where m_f and σ_f are the local mean and standard deviation of $f(k)$, and $w(k)$ is zero-mean white noise with unit variance. m_f can be estimated using the local mean of $g(k)$, so $f(k)$ can also be viewed as zero-mean Gaussian signal after m_f is subtracted. For the convenience of analysis, we drop m_f afterwards. It will not affect the result of the difference between $f(k)$ and its estimation $\hat{f}(k)$.

Accordingly, $f(k) \sim N(0, \sigma_f^2(k))$, $v(k) \sim N(0, \sigma_v^2)$, then $g(k) = f(k) + v(k) \sim N(0, \sigma_g^2(k))$, where $\sigma_g^2(k) = \sigma_f^2(k) + \sigma_v^2$. σ_v^2 depends on the quality of the image and usually can be regarded as a constant for the whole image. $\sigma_g^2(k)$ can be estimated using the following formula:

$$\hat{\sigma}_g^2(k) = \frac{1}{M}\sum_{i \in N(k)} g^2(i), \tag{6}$$

where $N(k)$ is the local neighborhood around k, M is the number of pixels within $N(k)$. According to the minimum mean square error (MMSE) criterion [10], the output of the Mihcak filter can be written as:

$$\hat{f}(k) = \frac{\hat{\sigma}_g^2(k) - \sigma_v^2}{\hat{\sigma}_g^2(k)} g(k) = (1 - Q(k))\, g(k), \tag{7}$$

where

$$Q(k) = \frac{\sigma_v^2}{\hat{\sigma}_g^2(k)} = \frac{M\sigma_v^2}{\sum_{i \in N(k)} g^2(i)}. \tag{8}$$

We use $Error(k)$ to represent the expectation of squared error at index k:

$$\begin{aligned} &Error(k) \\ &= E\left[\left(f(k) - \hat{f}(k)\right)^2\right] \\ &= E\left[\left(g(k) - v(k) - (1 - Q(k))g(k)\right)^2\right] \\ &= E\left[\left(Q(k)g(k) - v(k)\right)^2\right] \\ &= E\left[Q^2(k)g^2(k) - 2Q(k)(f(k) + v(k))v(k) + v^2(k)\right]. \end{aligned} \tag{9}$$

$v(k)$ and $f(k)$ only account for the center pixel of the neighborhood where $Q(k)$ is calculated, and $v(k)$ is independent of $f(k)$, so we assume that $Q(k)$, $f(k)$ and $v(k)$ are mutually independent to simplify the following deduction. Hence, Equation (9) can be simplified as:

$$
\begin{aligned}
&Error(k)\\
&= E[Q^2(k)]E[g^2(k)] - 2E[Q(k)]E[v^2(k)] + E[v^2(k)]\\
&= \sigma_g^2(k)E[Q^2(k)] + \sigma_v^2(1 - 2E[Q(k)]).
\end{aligned} \tag{10}
$$

If we let $X(k) = \sum_{i\in N(k)} (g(i)/\hat{\sigma}_g(k))^2$, it conforms to Chi-square distribution with a degree of M, $\chi^2(M)$. Here $\hat{\sigma}_g^2(k)$ is viewed as constant within $N(k)$. Therefore, $Y(k) = 1/X(k) \sim Inverse - \chi^2(M)$. We have

$$
\begin{cases}
E[Y(k)] = \dfrac{1}{M-2} (for \quad M > 2)\\
E[Y^2(k)] = \dfrac{1}{(M-2)(M-4)} \quad (for \quad M > 4)
\end{cases}. \tag{11}
$$

We rewrite Equation (8) using $Y(k)$:

$$
Q(k) = \frac{M\sigma_v^2}{\hat{\sigma}_g^2(k)} Y(k). \tag{12}
$$

Therefore,

$$
\begin{cases}
E[Q(k)] = \dfrac{M\sigma_v^2}{(M-2)\hat{\sigma}_g^2(k)}\\
E[Q^2(k)] = \dfrac{M^2\sigma_v^4}{(M-2)(M-4)\hat{\sigma}_g^4(k)}
\end{cases}. \tag{13}
$$

If the smallest neighbor we consider is $M = 3 \times 3$, substituting $E[Q(k)]$ and $E[Q^2(k)]$ in Equation (10) with Equation (13) yields:

$$
\begin{aligned}
&Error(k)\\
&= \frac{M(8-M)\sigma_v^4}{(M-2)(M-4)\hat{\sigma}_g^2(k)} + \sigma_v^2 \quad (for \quad M \geq 9).
\end{aligned} \tag{14}
$$

Our purpose is to abandon those coefficients severely contaminated by the denoising filter and keep the remaining ones. Therefore, we choose a threshold T, so that $Error(k) \leqslant T$. We set T to be proportional to the noise variance σ_v^2, i.e., $T = \lambda\sigma_v^2$. Obviously, $0 < \lambda < 1$. Therefore,

$$
\begin{aligned}
&\frac{M(8-M)\sigma_v^4}{(M-2)(M-4)\hat{\sigma}_g^2(k)} + \sigma_v^2 \leqslant \lambda\sigma_v^2\\
&\Rightarrow \hat{\sigma}_g^2(k) \leqslant \frac{M(M-8)}{(M-2)(M-4)(1-\lambda)}\sigma_v^2.
\end{aligned} \tag{15}
$$

where M is the neighborhood size of the Mihcak filter, and σ_v^2 is the power of noise. Once the Mihcak filter is applied, M and σ_v^2 are determined for a given signal, so λ is the only parameter needs to be specified. We will investigate the effect of different λ on the performance in Section III-B.

C. Proposed Scheme

Based on the above analysis, our method consists of two main steps: *Selection* and *Enhancement*. In the selection step, we only keep those coefficients with lower local variance in the wavelet representation of SPN and abandon the rest to alleviate or remove the influence of denoising errors. The remaining coefficients will be further enhanced to suppress the interference from scene details. These two steps aim to increase the identification performance by improving the SNR of extracted SPN. The details of the proposed filtering distortion removal are listed as follows:

1. ***Selection***: Transform every query image onto the wavelet domain, keep those wavelet coefficients with lower local variance (i.e. $\hat{\sigma}_g^2(k) \leq M(M-8)/(M-2)(M-4)(1-\lambda)\sigma_v^2$), and set the ones with higher local variance to 0;
2. ***Enhancement***: For those selected coefficients, use the models proposed in [5] to further restrain the scene details. To our experience, Model 3 with $\alpha = 6$ in [5] can achieve better identification rate (or equivalent) than other models;
3. ***Correlation***: Transform the wavelet coefficients back onto the spatial domain and calculate the correlation with the reference pattern noise according to Equation (2). Notice that the reference pattern noise is first represented in the wavelet domain and only the coefficients at the selected locations are preserved.

III. Experiments

A. Experimental Setup

The proposed scheme was compared with some existing works [1], [2], [5] on an image database consisting of 2,000 images taken by 10 cameras (each responsible for 200 images). The 10 cameras are Olympus C730UZ, Canon IXUS850IS, Canon PowerShotA400, Canon IXY500, FujiFilm Finepix S602, FujiFilm Finepix A920, Canon Ixus55, Olympus S1050SW, Samsung L74Wide and Samsung NV15. The first 6 cameras are owned by ourselves, but the last 4 cameras were randomly selected from the Dresden Image Database [12]. For each camera, another 50 blue-sky or flat-filed images were used to construct the reference SPNs.

For the sake of convenience, we will refer to [1] as "Basic", [2] as "MLE", and [5] as "Enhancer". To distinguish the impacts of selection and enhancement, we will show the results of only applying the *Selection*, and applying both the *Selection* and *Enhancement*, which will be referred to as "FDR 1" and "FDR 2", respectively. For the method in [1], we used the source code published in [13], [14]. For Li's approach [5], we used Model 3 with $\alpha = 6$ because it shows better results than his other models. In addition, for all the methods involved, we used image blocks cropped from the center of the green channel of the full-size color images. For the fairness of comparison, we set $M = 25$ and $\sigma_v^2 = 9$ for all the methods that use the Mihcak filter. It is also worth mentioning that the reference SPNs constructed by different methods will be processed by SEA [7] to suppress the periodic artifacts before calculating the correlations using Equation (3).

B. Performance Evaluation

We used the overall ROC to compare the performances of different methods. To obtain the overall ROC curve, for a given detection threshold, the numbers of true positives and false positives are counted for each camera, respectively, then these numbers are summed up and used to calculate the True Positive Rate (TPR) and False Positive Rate (FPR). Specifically, as the numbers of images captured by each camera are exactly the same, we can simply calculate the TPR and FPR for a threshold as follows:

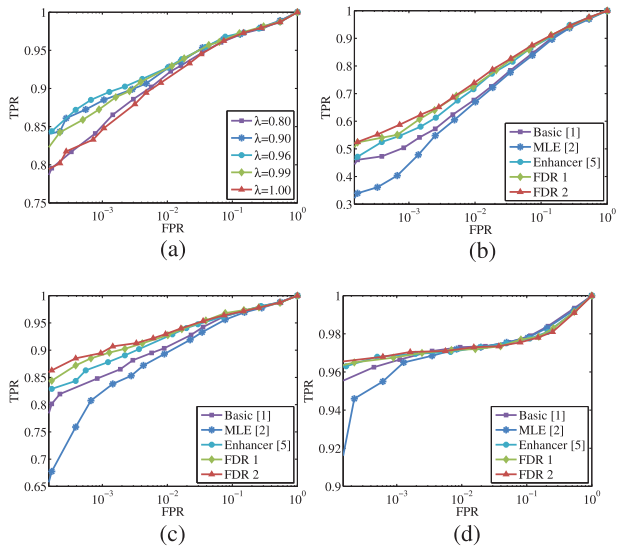

Fig. 1. Overall ROC curves for various image sizes and λ. (a) 256×256, $\lambda \in [0.8, 1.0]$ (b) 128×128, $\lambda = 0.96$ (c) 256×256, $\lambda = 0.96$ (d) 512×512, $\lambda = 0.96$.

$$\begin{cases} \text{TPR} = \dfrac{\sum_{i=1}^{C} \mathcal{T}_i}{T} \\ \text{FPR} = \dfrac{\sum_{i=1}^{C} \mathcal{F}_i}{(C-1)T} \end{cases}, \tag{16}$$

where C is the number of cameras, T is the total number of query images, $\mathcal{T}_i$ and $\mathcal{F}_i$ are the true positives and false positives of camera i, respectively. In order to show the details of the ROC curves with a low FPR, all the ROC curves are plotted in the logarithmic scale.

To see how significantly λ affects the performance, we varied λ from 0.8 to 1.0 and showed the results on image blocks of 256×256 pixels in Fig. 1(a), where no enhancement is applied and $\lambda = 1.00$ means filtering distortion is not removed. As can be seen, the performance increases initially and then decreases as λ keeps falling down, which clearly shows that abandoning those coefficients that are severely contaminated helps improve the performance. Based on the experiments, a λ between [0.95,0.99] deliveries satisfactory results for different image sizes. In the following experiments, λ is fixed to 0.96. The comparisons with other methods on image blocks sized 128×128, 256×256 and 512×512 pixels are shown in Fig. 1(b), 1(c) and 1(d), respectively. While the improvement on images of 512×512 is not so significant as on images of 256×256 and 128×128 pixels, the performance of the filtering distortion removed SPN is better than those of other methods that do not take the denoising errors into consideration. Furthermore, the performance of FDR 2 is better than that of FDR 1, which means enhancing the selected SPN can further improve the performance by attenuating the influence of scene details. But as shown in Fig. 1(d), enhancement helps very little in boosting the performance on large image blocks sized 512×512 pixels.

The TPRs of 5 methods at a low FPR of 5×10^{-4} are shown in Table I, which demonstrates that the TPR of FDR 1 is $2\% \sim 14\%$, $3\% \sim 10\%$ and $1\% \sim 2\%$ higher than those of [1], [2], [5] on images of 128×128, 256×256 and 512×512 pixels, respectively. Besides, the performance can be slightly improved via further enhancing the selected SPN. Similar to the main tendencies observed in Fig. 1, it seems that the smaller the image size, the higher the improvement. This is probably due to the fact that, when compared with the relatively less SPN information that is available in smaller images, the improved quality of SPN by removing the filtering distortions is more notable and therefore boosts the performance more significantly. To see how many "clean" wavelet coefficients have been retained, we drew the distribution of the percentages of the selected wavelet coefficients for 2,000 images in Fig. 2. As can be observed, by specifying $\lambda = 0.96$, around $80\% \sim 90\%$ of the wavelet coefficients are selected for for most images sized 128×128 and 256×256 pixels. Note that the selection scheme does not cost extra computation, because the local variance $\hat{\sigma}_g^2(k)$ is already available when performing the Mihcak filtering [10].

TABLE I
THE TPRS OF 5 METHODS AT A LOW FPR OF 5×10^{-4}

Sizes	Basic [1]	MLE [2]	Enhancer [5]	FDR 1	FDR 2
128×128	0.4730	0.3705	0.5250	**0.5405**	**0.5520**
256×256	0.8195	0.7715	0.8435	**0.8720**	**0.8850**
512×512	0.9625	0.9460	0.9630	**0.9650**	**0.9650**

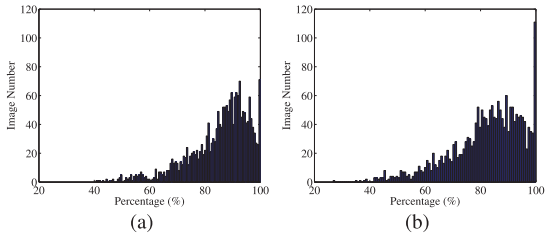

Fig. 2. The distribution of the percentages of the selected wavelet coefficients for images sized (a) 256×256 and (b) 128×128 pixels when setting $\lambda = 0.96$.

IV. CONCLUSIONS

In this paper, we propose a method of obtaining better SPN for source camera identification. We contended that part of the SPN may have been contaminated by the denoising filter errors. By analyzing the Mihcak denoising filter [10], we discovered that the errors are closely related to the local variances of wavelet coefficients. Accordingly, the quality of the SPN is improved by abandoning the wavelet coefficients with higher local variances. The filtering distortion removed SPN is then further enhanced using Li's models to restrain the scene details. Compared with some existing approaches that apply the Mihcak filter, our method achieves better identification performance in terms of the overall ROC curves. Despite better denoising filters, such as the PCAI [15] and the BM3D algorithm [16], have been proposed to extract SPN, but the entire denoising processes of them are much more complicated. Therefore, we will leave the analysis of the denoising errors of other SPN extractors to our future work. Additionally, as some useless SPN components have been discarded, the proposed scheme can serve as a dimensionality reduction method potentially, which would be another direction of our future work.

REFERENCES

[1] J. Lukas, J. Fridrich, and M. Goljan, "Digital camera identification from sensor pattern noise," *IEEE Trans. Inf. Forensics Secur.*, vol. 1, no. 2, pp. 205–214, 2006.

[2] M. Chen, J. Fridrich, M. Goljan, and J. Lukás, "Determining image origin and integrity using sensor noise," *IEEE Trans. Inf. Forensics Secur.*, vol. 3, no. 1, pp. 74–90, 2008.

[3] Y. Hu, B. Yu, and C. Jian, "Source camera identification using large components of sensor pattern noise," *Proc. Int. Conf. Computer Science and its Applications*, 2009, pp. 291–294.

[4] X. Kang, Y. Li, Z. Qu, and J. Huang, "Enhancing source camera identification performance with a camera reference phase sensor pattern noise," *IEEE Trans. Inf. Forensics Secur.*, vol. 7, no. 2, pp. 393–402, 2012.

[5] C.-T. Li, "Source camera identification using enhanced sensor pattern noise," *IEEE Trans. Inf. Forensics Secur.*, vol. 5, no. 2, pp. 280–287, 2010.

[6] C.-T. Li and Y. Li, "Color-decoupled photo response non-uniformity for digital image forensics," *IEEE Trans. Circuits Syst. Video Technol.*, vol. 22, no. 2, pp. 260–271, 2012.

[7] X. Lin and C.-T. Li, "Preprocessing reference sensor pattern noise via spectrum equalization," *IEEE Trans. Inf. Forensics Secur.*, vol. 11, no. 1, pp. 126–140, 2016.

[8] A. Cortiana, V. Conotter, G. Boato, and F. G. B. De Natale, "Performance comparison of denoising filters for source camera identification," *Proc. SPIE*, 2011, pp. 788 007–788 007–6.

[9] G. Chierchia, S. Parrilli, G. Poggi, C. Sansone, and L. Verdoliva, "On the influence of denoising in prnu based forgery detection," *Proc. 2nd ACM Workshop on Multimedia in Forensics, Security and Intelligence*, 2010, pp. 117–122.

[10] M. Mhak, I. Kozintsev, and K. Ramchandran, "Spatially adaptive statistical modeling of wavelet image coefficients and its application to denoising," *Proc. IEEE Int. Conf. Acoustics, Speech, and Signal Processing*, 1999, vol. 6, pp. 3253–3256.

[11] D. T. Kuan, A. A. Sawchuk, T. C. Strand, and P. Chavel, "Adaptive noise smoothing filter for images with signal-dependent noise," *IEEE Trans. Patt. Anal. Mach. Intell.*, no. 2, pp. 165–177, 1985.

[12] T. Gloe and R. Böhme, "The dresden image database for benchmarking digital image forensics," *J. Dig. Forensic Pract.*, vol. 3, no. 2–4, pp. 150–159, 2010.

[13] M. Goljan, J. Fridrich, and T. Filler, "Large scale test of sensor fingerprint camera identification," *Proc. SPIE*, 2009, pp. 72 540I–72 540I.

[14] Camera Fingerprint-Matlab implementationm online. [Available]: http://dde.binghamton.edu/download/camera_fingerprint/, 2012.

[15] X. Kang, J. Chen, K. Lin, and P. Anjie, "A context-adaptive spn predictor for trustworthy source camera identification," *EURASIP J. Image Video Process.*, vol. 2014, no. 1, pp. 1–11, 2014.

[16] K. Dabov, A. Foi, V. Katkovnik, and K. Egiazarian, "Image denoising by sparse 3-d transform-domain collaborative filtering," *IEEE Trans. Image Process*, vol. 16, no. 8, pp. 2080–2095, 2007.